QA: QA

Civilian Radioactive Waste Management System
Management & Operating Contractor

Waste Package Related Impacts of Plutonium Disposition Waste Forms in a Geologic Repository

TDR-EBS-MD-000003 REV 01 ICN 01

January 2000

Prepared for:

U.S. Department of Energy
Office of Civilian Radioactive Waste Management
1000 Independence Avenue SW
Washington, D.C. 20585

Prepared by:

Civilian Radioactive Waste Management System
Management & Operating Contractor
1211 Town Center Drive
Las Vegas, Nevada 89144

Under Contract Number
DE-AC08-91RW00134

3. STRUCTURAL ANALYSIS

3.1 MOX

The structural design criteria for the 12 and 21 PWR waste packages containing MOX SNF are given in Section 2.1.5.1, with which the results in this section comply. For the criteria evaluated, the tipover accident produces the highest stresses in the waste package since the upper part of the waste package experiences a drop greater than the two-meter criteria. Analyses were performed for the 21 PWR MOX WP (CRWMS M&O 1998h) and 12 PWR MOX WP (CRWMS M&O 1998i) to determine the structural response to a tipover accident design basis event (DBE) dynamic load (CRWMS M&O 1997i, p. 44).

3.1.1 Structural Analysis Method

A three-dimensional finite-element solution was performed by making use of the ANSYS V5.4 finite-element computer code (CSCI: 30040 V5.4) (CRWMS M&O 1998j). ANSYS is qualified as documented in the SQR (CRWMS M&O 1998j). A finite-element representation of the waste package was developed to determine the effects of tipover accident DBE loads on the waste package structural components. The basket structure in the 21 PWR MOX WP was represented with B-SS absorber plates and a combination of A 516 carbon steel and aluminum in the basket structure. The aluminum serves as a heat conduit (thermal shunt) in the waste package and is not a structural material. The basket structure in the 12 PWR MOX WP was represented in a similar manner as the 21 PWR MOX WP except that two calculations were conducted on the waste package, one with and one without B-SS absorber plates. The waste package was represented with an initial orientation of 30° between the symmetry axis and vertical in order to initiate tipping of the waste package, and gravitational acceleration was then applied to the system. Having the waste package represented in this configuration, the simulation was continued throughout the impact until the waste package began to rebound, at which time the peak stresses have been obtained.

The MOX assembly weight is estimated to be 618.8 kg compared to 619.2 kg for the commercial Vantage 5 assembly (CRWMS M&O 1998k, p. 6). Weight changes due to burnup are negligible (less than 25 g at the maximum burnup). The structural analyses show that stresses from the tipover accident for both SNF waste forms are of similar magnitude.

3.1.2 Structural Analysis Results

The structural response of the waste package to tipover accident loads is given as maximum stress values obtained from the finite-element solutions to the problem. These solutions indicate that the maximum stress is located in the region of the inner and outer barrier lids in the vicinity of the impact region between the waste package and the target surface for 12 and 21 PWR waste package designs. The maximum membrane stress plus bending stress of the 21 PWR WP containing MOX SNF due to a tipover accident is 524 MPa in the inner barrier and the inner barrier lid (CRWMS M&O 1998h, p. 8 and Table 6-1) compared to 456 MPa for the 21 PWR WP containing LEU SNF (CRWMS M&O 1998l, p. 11). The maximum membrane stress plus bending stress of the 12 PWR WP containing MOX SNF due to a tipover accident is 404 MPa

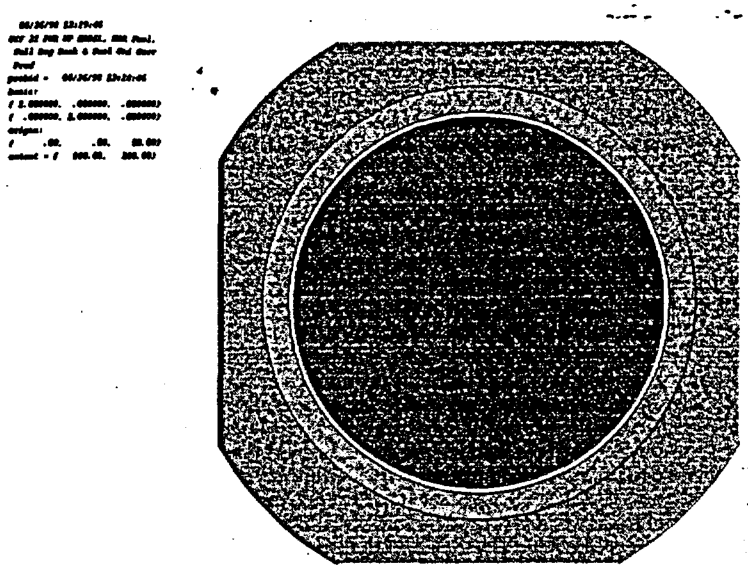

Figure 6-20. Fully Degraded Fuel and Basket Material Uniformly Distributed Throughout Interior Volume of 21 PWR WP

6.1.3.3.5 Criticality Results for Degraded Fuel and Fully Degraded Basket

Results of the criticality analyses of the 21 MOX PWR WP with a fully degraded basket, minimally spaced collapsed fuel rods (0.9144 cm), and a uniform corrosion product distribution are given in Table 6.3-1 of CRWMS M&O (1998c, p. 46). The maximum k_{eff} value was less than 0.675 for these cases, well below the critical limit of 0.92, as shown in Figure 6-21 (MOX labels). All values are for a rod center-to-center spacing of 0.9144 cm (rods touching in square lattice) representative of a nominal configuration. (Note: Nominal configuration; sensitivity to rod spacing is discussed below.) The ultra-conservative assumption (because of the low corrosion rate of zircaloy compared to carbon steel) that SNF degradation begins simultaneously with the baskets (see Section 6.3.2) is made in two of the analyses shown in Figure 6-21 (MOX Curves A and C). A more realistic SNF degradation assumption, where loss of the principal isotopes begins at 10,000 years after the start of basket degradation (MOX Curve B in Fig. 6-21), shows a moderate increase in k_{eff} over time relative to the early loss of the principle isotopes. Also of interest are the reduced peak-and-valley effect with time and the movement of the peak k_{eff} out to ~ 45,000 years. Both effects result from increased resonance absorption due to the harder spectrum of this configuration. The location of the peak shifts outward in time because the increased absorption in ^{240}Pu in a harder spectrum is not matched by an equal increase in ^{239}Pu fission. Thus, longer decay times are required to eliminate the absorption effect from ^{240}Pu.

Results from a similar analysis for the 21 LEU PWR WP (fully degraded baskets, minimally spaced collapsed fuel rods, and uniform corrosion products) (CRWMS M&O 1998p, Section 6) are also shown in Figure 6-21 with the LEU labels. This case utilized the 4.0 wt% ^{235}U, 35.0 GWd/MTU LEU SNF with a 1.0922 cm square pitch (normal pitch is 1.44272 cm). The MOX SNF k_{eff}s were less than those from the similar LEU SNF cases; the maximum LEU SNF k_{eff} was approximately 0.7.

these runs is actually controlled by other silicates (clays, zeolites or Ni_2SiO_4) during the times of greatest U-silicate deposition (CRWMS M&O 2000b, Section 6.1).

Group 8: This single case (8) tests the effect of changing the saturation to only 10% of the void space of the porous invert (all other cases assume 100% saturation). The flow out of the WP is spread evenly over the footprint of the WP, since the spreading of flow out of the waste package is consistent with the lower saturation. Effectively, this case increases the mass and surface area of invert minerals seen by the fluid that passes through the invert. However, it also decreases the residence time of the fluid in the invert. Compared to 1a, Pu deposition is reduced by a factor ~8, but U deposition in the invert is approximately the same (CRWMS M&O 2000b, Section 6.1).

Group 9: This group (9o6^, 9o6, 9o7, and 9o8) provides a sensitivity study on the importance of the Pu-ceramic corrosion rate. The first of these cases (9o6^) can be compared with case 6 (pre-decay the ^{239}Pu to ^{240}U over one half-life of ^{239}Pu, 24,100 years). The other three cases can be compared with 4ao. It is seen that the increase in Pu deposition varies almost linearly with the increase in ceramic corrosion rate, up to a factor 10 increase in the corrosion rate. At corrosion rates higher than 10x, the aqueous Pu concentration in the WP source term becomes mass-limited. These results are expected. As outlined above, the Pu concentration in the WP source term is expected to vary almost linearly with ceramic corrosion rate (since no Pu solid precipitates in the WP during the time of peak Pu loss). In addition, the invert conditions are so out of equilibrium with the source term, that almost every bit of Pu that enters the invert precipitates (CRWMS M&O 2000b, Section 6.1). The cases with pre-decay of Pu are useful for simulating the effect of the delay of waste package breach. As explained in Section 7.4, the decay of Pu-239 to U-235 reduces the criticality of the waste package because the latter is less efficient than the former at neutron fission.

Group 10: This group tests the effects of increasing the amount of diluting J-13-like water added to the invert (by diversion around the WP, as discussed in Section 5.4 of Ref 3); the cases may be compared with 2u. The flow out of the WP is not focussed; that is, it is spread evenly over the footprint of the WP. The effect of increasing the dilution by a factor of 100 is remarkably small (CRWMS M&O 2000b, Section 6.1).